Pergamon

Journal of Structural Geology, Vol. 18, No. 12, pp. 1487 to 1491, 1996

PII: S0191-8141(96)00055-7
0191-8141/96 $15.00 + 0.00

Computer modelling of mantled porphyroclasts in Newtonian and non-Newtonian simple shear viscous flows

TOSHIAKI MASUDA and NAOYA MIZUNO*

Institute of Geosciences, Shizuoka University, Shizuoka 422, Japan

(*Received* 12 *December* 1995; *accepted in revised form* 30 *June* 1996)

Abstract—In computer simulations based on creeping motion equations, the difference in stress sensitivity of strain rate between Newtonian rheology and non-Newtonian power-law rheology does not greatly influence the types of mantled porphyroclast developed in simple shear viscous flows. Porphyroclast type is determined by the radius of an initial spherical mantle. When a thin mantle lies within the separatrix, δ_2-objects develop at small γ, then complex porphyroclasts appear with increasing γ. When the mantle is thicker and transected by the separatrix, ϕ-objects form at small γ and δ_2-objects appear with increasing γ during the same deformation. The transition from ϕ- to δ_2-objects is gradual, the transition strain being dependent on the initial radius of the mantle. Our simulations did not produce θ-, δ_1- or σ-objects. Copyright © 1996 Elsevier Science Ltd

INTRODUCTION

Porphyroclasts are potentially very useful for deformation analysis in mylonites. Since Passchier & Simpson (1986) emphasised their usefulness, mantled porphyroclasts have been confidently used as a shear sense indicator (Choukroune *et al.* 1987, Mawer 1987, Van Den Driessche & Brun 1987, Hooper & Hatcher 1988, Hanmer & Passchier 1991, Simpson & De Paor 1993). Recently, Passchier *et al.* (1993) and Passchier (1994) proposed a genetic model that shows how various mantled porphyroclasts develop in relation to patterns of flow perturbations around porphyroclasts. Passchier *et al.* (1993) divided δ-type porphyroclasts into two subtypes: one without stair-stepping wings and one with stair-stepping wings. Here we denote the former as a δ_1-object and the latter as a δ_2-object. They attributed the difference in the shape of the wings to the difference in flow perturbations, which can be 'eye shaped' or 'bow-tie shaped' separatrices (Passchier *et al.* 1993, p. 241, connections 3 and 4 in Table 1), to the stress sensitivity of strain rate in the matrix during Newtonian or non-Newtonian flows (connections 1 and 2 in Table 1). Passchier (1994) subsequently proposed a more advanced model that explains how σ-type, ϕ-type and θ-type porphyroclasts develop. This new model is also based on the shape of the separatrix and the stress sensitivity of strain rate, and introduced a new factor, the geometrical relationship between initial mantle material and the separatrix (Table 1).

These models are based on theoretical analyses of flow perturbations within Newtonian viscous material (Masuda & Ando 1988, Bjornerud 1989), and seem to be supported by experimental results on non-Newtonian viscous materials (Passchier & Sokoutis 1993) and rock analogues (ten Brink & Passchier 1995). However, in these experiments, deformation was produced in annular shear zones where strain rate gradients are intrinsically present (Masuda *et al.* 1995). Thus, these experimental results may not be valid for straight and parallel-sided shear zones in nature. Masuda & Mizuno (1996) theoretically analysed non-Newtonian, power-law viscous flows around a rigid cylinder, and revealed that a 'double-bulge shaped' separatrix occurs in both Newtonian and non-Newtonian viscous flows. This means that connections 1 and 2 in Table 1 may be suspect. In this paper we produce numerically various mantled porphyroclasts in Newtonian and non-Newtonian simple shear flows, aiming at testing the model by Passchier (1994). Unfortunately, our results do not agree with this model; we propose a new scheme (Table 2).

NEWTONIAN MATRIX

Boundary conditions for simulation

We consider bulk simple shear flow of a viscous material containing a rigid spherical inclusion: the viscous material and rigid spherical body simulate the flowing matrix of rocks and an unstrained porphyroclast, respectively. We assume that the matrix material is incompressible and that the deformation is very slow and not time-dependent. We also assume no slip or detachment between the spherical body and the matrix, and no volume loss during deformation.

Theoretical analysis

Velocity vectors around the sphere have been previously solved in different ways (Einstein 1956, Oertel 1965, Wakiya 1956, Cox *et al.* 1968, Masuda & Ando 1988, Bjornerud 1989, Gray & Busa 1994). Here we follow the solution proposed by Masuda & Ando (1988). They give the approximate velocity vector (u, v, w) at (x, y, z) of the Cartesian coordinates by polynomial functions, the shear plane being perpendicular to the z-axis and shear direction parallel to the x-axis. The radius

*Present address: Geology Division, CTI Engineering Co., Ltd, Nihonbashi Honcho, Tokyo 103, Japan.

SG 18:12-G

Table 1. Models for mantled porphyroclasts in terms of flow perturbations and stress-sensitivity of strain rate compiled after Passchier *et al.* (1993) and Passchier (1994). We here denote the δ-object without stair-stepping wings as δ_1-object and that with stair-stepping wings as δ_2-object, respectively. The Passchier (1994) model consists of four genetic connections that are tied by numbered arrows. For explanation see text

Rheology		Separatrix		Relationship between mantle and separatrix		
				(1) mantle in separatrix	(2) separatrix intersects mantle	(3) separatrix in mantle
Newtonian	$\leftrightarrow^1$	'eye'	$\leftrightarrow^3$	θ-object	δ_1-object	ϕ-object
non-Newtonian	$\leftrightarrow^2$	'bow-tie'	$\leftrightarrow^4$	θ-object	δ_2-object	σ-object

of the central sphere is set as 1. We use their velocity vector where $|x| \leq 5$ where the flow is strongly perturbed, while we assume the following velocity where $|x| > 5$:

$$u = \dot{\gamma}z + 0.5\dot{\gamma}z(x^2 + z^2)^{-3/2}$$
$$v = 0$$
$$w = -0.5\dot{\gamma}x(x^2 + z^2)^{-3/2}$$

This velocity represents the sum of velocities influenced by a rotating sphere and those of the simple shear flow. The sphere rotates with an angular velocity of $\dot{\gamma}/2$ where $\dot{\gamma}$ is the shear strain rate (Jeffery 1922).

Although the theory is three dimensional, we deal, for brevity, with the flow on a two-dimensional section perpendicular to the bulk shear plane and parallel to the shear direction of the far-field flow that cuts the centre of the rigid sphere (the x–z plane). Since observations of natural mantled porphyroclasts are usually made on this plane, our analysis is reasonable.

Separatrix

A Newtonian viscous matrix has a 'double-bulge shaped' separatrix when the bulk deformation is simple shear (Cox *et al.* 1968, Masuda & Mizuno 1996). The separatrix separates domains of open and closed particle paths: particles within the separatrix have ovoid orbits around the sphere, whereas those outside the separatrix flow away from the sphere.

Following Cox *et al.* (1968), we introduce ρ_{min} and ρ_{max} which are defined as the minimum and maximum distance of the particle on the path from the centre of the sphere. The open paths have a finite ρ_{min} and infinite ρ_{max}, whereas the closed paths have finite ρ_{min} and ρ_{max}. The separatrix has a finite ρ_{min} ($1.14 < \rho_{min} < 1.15$) but infinite ρ_{max} (Cox *et al.* 1968, Masuda & Mizuno 1996). This scheme is different from Passchier *et al.* (1993) and Passchier (1994), their separatrix having finite ρ_{min} and ρ_{max}.

Model of mantled porphyroclast

The mantle of the porphyroclasts is modeled by a material with the same rheological properties as the matrix. Thus, it behaves as a passive marker in the matrix during deformation. The mantle material was initially set circular. It was assumed, as previously mentioned, that no volume change of the mantle and the sphere occurred during deformation (cf. Passchier & Simpson 1986, Bjornerud & Zhang 1995).

Results

The movement of the mantle material is traced by Euler's method (e.g. Mathews 1987) using data from the velocity vector field. Its shape gradually changes with progressing far-field simple shear (γ) to develop wings, exhibiting more complex shapes at high strains. The length of the two wings are slightly different. This is an artifact of the numerical approximations inherent in the solution. Figures 1–3 show how the mantled porphyroclasts develop for 5 different cases of initial radius of mantle (R). The simulation was restricted to $\gamma \leq 14$, and the sphere rotates 401° during this period. The types of simulated mantled porphyroclasts are tabulated in Table 2.

Thin mantle in the separatrix (R = 1.13 *of Figs.* 1 & 2)

Since all of the mantle material is in the separatrix, no material crosses the separatrix into the domain of far field flow. The mantle exhibits clear wings by $\gamma = 4$. The length of the wings becomes longest at around $\gamma = 8$, where the ends of the wings are close to the centre line. These

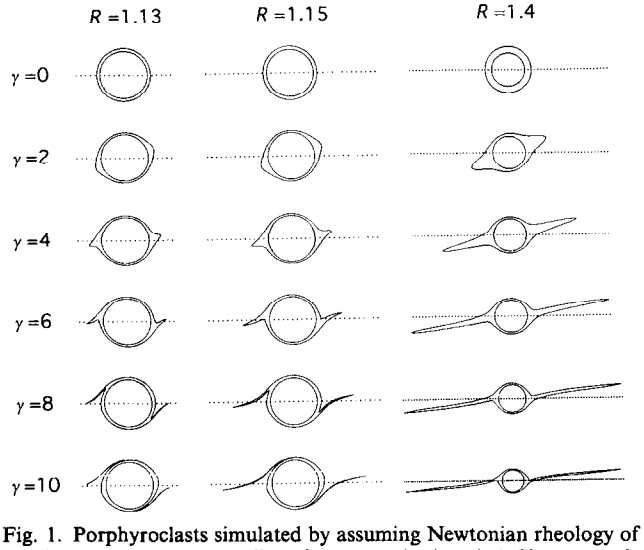

Fig. 1. Porphyroclasts simulated by assuming Newtonian rheology of matrix around a sphere. Radius of the central sphere is 1. Shear sense is dextral. The mantle with $R = 1.13$ is in the separatrix, whereas those with $R = 1.15$ and 1.4 are transected by the separatrix.

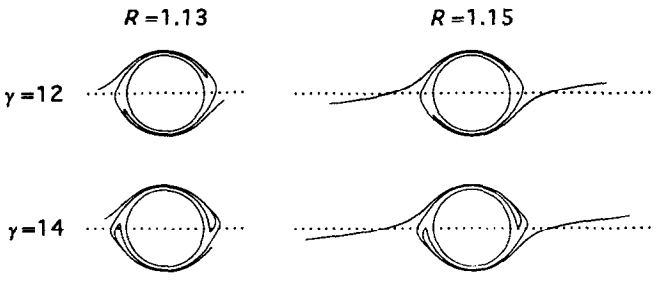

Fig. 2. Selected examples showing development of 'lagoons'. Shear sense is dextral. The mantle with $R=1.13$ is in the separatrix, whereas that with $R=1.15$ is transected by the separatrix.

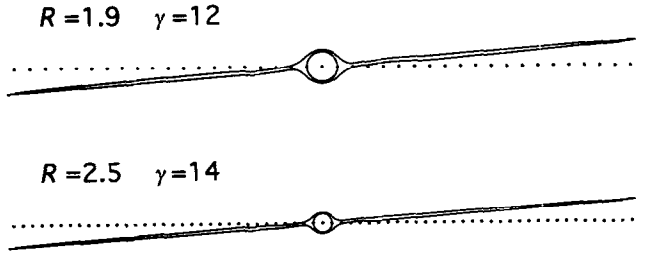

Fig. 3. Selected examples of porphyroclasts with extremely long wings at larger strains. These are ϕ-objects. Shear sense is dextral. The symmetric axes of the objects are oblique to the shear plane.

mantled porphyroclasts were assigned to the δ_2 class by their appearance. With increasing γ, the wings become thinner and appear to be rolled up by the rotating sphere. Embayment of the matrix material becomes prominent by $\gamma=6$. It becomes much more prominent up to $\gamma=10$. At $\gamma=14$, the embayed matrix material appears to have accumulated to form 'lagoons' at opposite sides of the sphere on the centre line. Passchier (1994) predicted θ-objects in this situation (Table 1), which have no wings. Our result does not support his model.

Mantle transected by the separatrix (Figs. 1–3)

Mantle material outside the separatrix will move away from the sphere, whereas those within the separatrix never escape from this structure. Such a complex flow simultaneously produces wings of mantle material outside the separatrix and causes embayment of the matrix material within the separatrix. When the initial radius of the mantle is small ($R=1.15$ in Figs. 1 & 2), the ϕ-object appears only at very low strains (e.g. $\gamma=2$), its symmetric axis being oblique to the centre line. An asymmetric appearance of the mantle becomes clear at $\gamma=4$, and a δ_2-object forms by $\gamma=6$. The transition from ϕ- to δ_2-objects is not sharp. Stair-stepping wings are obvious at this strain. The wings become thinner and longer at larger strains. The embayment of the matrix is prominent at $\gamma\geq 8$, and the embayed matrix forms 'lagoons' by $\gamma=14$ (Fig. 2).

As the initial radius of mantle increases ($R=1.4$, 1.9 and 2.5 of Figs. 1 & 3), the manner of mantle development changes gradually: the embayment of the matrix material occurs at higher strains and becomes less prominent while the wings becomes more prominent at lower strains for larger mantles. Embayment of matrix materials is ambiguous and no 'lagoons' are visible at $\gamma=14$ when the initial radius of the mantle is 1.9 and 2.5 (Fig. 3). The transition from ϕ- to δ_2-objects takes place at larger strains when R is larger. In these cases, the ϕ-object survives up to strains of $\gamma=12$ and 14, respectively. Passchier *et al.* (1993) and Passchier (1994) predicted a δ_1-object in this situation, but the simulation produced a δ_2-object and a ϕ-object at earlier stages of strain.

NON-NEWTONIAN VISCOUS MATRIX

Power-law flow

Power-law flow is usually represented by a relationship between the one-dimensional stress (τ) and the strain rate component ($\dot{\gamma}$) by $\dot{\gamma}\propto\tau^n$, where n is the stress exponent. If $n=1$, the material exhibits Newtonian viscosity. The magnitude of n has been determined to be 3–5 for some minerals and rocks through high temperature, high pressure deformation experiments (Nicolas & Poirier 1976, Kirby & McCormick 1984, Poirier 1985, Tsenn & Carter 1987).

Two dimensional analysis

We used the velocity vectors obtained by Masuda & Mizuno (1996) for power-law simple shear flow up to

Table 2. A new scheme for mantled porphyroclasts in terms of flow perturbations up to $\gamma=14$ and 10 for Newtonian and non-Newtonian matrix, respectively. A vertical arrow indicates an increase in simple shear strain. ϕ-objects at low values of γ are omitted in column (1) for both Newtonian and non-Newtonian flows, because they are transient. The difference between a Newtonian and non-Newtonian matrix has no influence on the type of resulting mantled porphyroclasts

				Relationship between mantle and separatrix	
Rheology		Separatrix		(1) mantle in separatrix	(2) separatrix intersects mantle
Newtonian	↔	'double bulge'	↔	δ_2-object ↓ complex	ϕ-object ↓ δ_2-object
non-Newtonian	↔	'double bulge'	↔	δ_2-object ↓ complex	ϕ-object ↓ δ_2-object

$n = 5$. Since their analysis was essentially two dimensional, their rigid inclusion was a cylinder with an infinite length instead of a sphere in three dimensions. The other assumptions for calculation in their non-Newtonian analysis were the same as those taken for Newtonian analysis (very slow, time-independent flow; no slip movement between the rigid material and the matrix; no volume change during deformation). Notable results of Masuda & Mizuno (1996) were that (1) the angular velocity of the cylinder was equal to $\dot{\gamma}/2$ irrespective of n, which is exactly the same as that obtained by Jeffery (1922) for a sphere embedded in a Newtonian viscous matrix, (2) a 'double-bulge shaped' separatrix occurs even in power-law flows around a rigid cylinder, its size being inversely proportional to n, and (3) patterns of velocity vectors, deflection of marker particles and distributions of dynamic and kinematic quantities (pressure, differential stress, strain rate, kinematic vorticity number etc.) are similar for different n as a first approximation.

Results

We analysed three cases of initial mantle radius ($R = 1.05$, 1.1 and 1.3) in the same way as the Newtonian flow up to $\gamma = 10$, and the cylinder rotates 287° during this period. We present results for $n = 5$ in Fig. 4, the types of objects generated being tabulated in Table 2. Since $1.05 < \rho_{min} < 1.06$ for the separatrix at $n = 5$ (Masuda & Mizuno 1996), the mantle with $R = 1.05$ (Fig. 4, left) is in the separatrix. Those with $R = 1.1$ (centre) and 1.3 (right) are transected by the separatrix. The types of objects generated for $n = 2$, 3 and 4 (not shown) are essentially the same as those for $n = 5$. They are also the same as those produced in Newtonian flow (compare Fig. 4 with Figs. 1 & 2 and see Table 2), although the precise geometry of mantles at each stage of strain is a little different from those produced during the Newtonian analyses at equivalent strains.

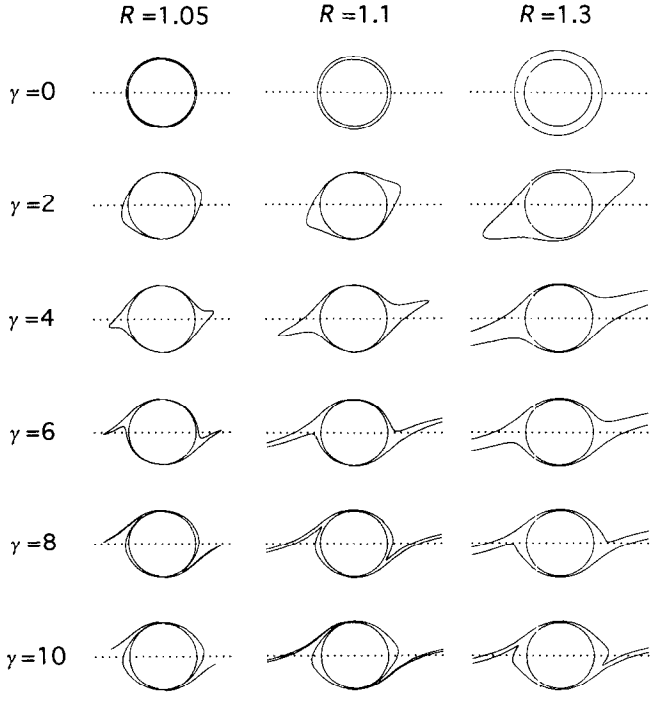

Fig. 4. Simulated porphyroclasts ($|x| < 2.6$) around a cylinder within non-Newtonian power-law matrix of $n = 5$. Shear sense is dextral. The mantle with $R = 1.05$ is in the separatrix, whereas those with $R = 1.1$ and 1.3 are transected by the separatrix.

DISCUSSION

We could not produce σ, θ and δ_1-objects with this analysis, although they were listed in the original model (Table 1). Since these objects are commonly present in natural shear zones, our simulation is obviously incomplete. Other factors, which we did not consider here, must influence the development of these objects. Passchier (1994) presented atypical, complex porphyroclasts and listed the main causes of deviation from typical porphyroclasts: (1) a shrinking porphyroclast adding material to the mantle, (2) a non spherical porphyroclast, (3) a non passive mantle, and (4) deviation from simple shear. Bjornerud & Zhang (1995) added a further factor (5) variation in coupling between the sphere and the mantle. These 5 factors should be critically examined to see if they are the main causes for the development of σ-objects, ϕ-objects and δ_1-objects. In any case, the genesis of mantled porphyroclasts is undoubtedly more complicated than suggested by Passchier *et al.* (1993) and Passchier (1994).

Acknowledgements—The manuscript was revised when the senior author was at James Cook University. We thank Tim Bell for constructive comments and critical reading of the early version of the manuscript, and Ken Hickey and Cees Passchier for stimulating discussions. We also thank Norman Gray and Chris Mawer for helpful comments and Richard Norris for kind editing of the manuscript.

REFERENCES

Bjornerud, M. 1989. Mathematical model for folding of layering near rigid objects in shear deformation. *J. Struct. Geol.* **11**, 245–254.

Bjornerud, M. G. & Zhang, H. 1995. Flow mixing, object-matrix coherence, mantle growth and the development of porphyroclast tails. *J. Struct. Geol.* **17**, 1347–1350.

Choukroune, P., Gapais, D. & Merle, O. 1987. Shear criteria and structural symmetry. *J. Struct. Geol.* **9**, 525–530.

Cox, R. G., Zia, Y. Z. & Mason, S. G. 1968. Particle motions in sheared suspensions. XXV. Streamline around cylinders and spheres. *J. Colloid Interface Sci.* **27**, 7–18.

Einstein, A. 1956. *Investigations on the Theory of the Brownian Movement* (edited by Furth, R.). Dover, New York.

Gray, N. H. & Busa, M. D. 1994. The three-dimensional geometry of simulated porphyroblast inclusion trails: inert-marker, viscous-flow models. *J. Metamorph. Geol.* **12**, 575–587.

Hanmer, S. & Passchier, C. W. 1991. Shear-sense indicators: a review. Geological Survey of Canada Paper 90-17.

Hooper, R. J. & Hatcher, R. D. 1988. Mylonites from the Towaliga fault zone, central Georgia: products of heterogeneous non-coaxial deformation. *Tectonophysics* **152**, 1–17.

Jeffery, G. B. 1922. The motion of ellipsoidal particles immersed in a viscous fluid. *Proc. R. Soc. Lond., Ser. A* **102**, 161–179.

Kirby, S. H. & McCormick, J. 1984. Inelastic properties of rocks and minerals: strength and rheology. In: *CRC Handbook of Physical Properties of Rocks*, Vol. III (edited by Carmichael, R. S.). CRC Press, Boca Raton, 140–280.

Masuda, T. & Ando, S. 1988. Viscous flow around a rigid spherical body: a hydrodynamic approach. *Tectonophysics* **148**, 337–346.

Masuda, T. & Mizuno, N. 1996. Deflection of non-Newtonian simple

shear flow around a cylindrical body by the Finite Element Method. *J. Struct. Geol.* **18**, 1089–1100.

Masuda, T., Mizuno, N., Kobayashi, M., Nam, T. N. & Otoh, S. 1995. Stress and strain estimates for Newtonian and non-Newtonian materials in a rotational shear zone. *J. Struct. Geol.* **17**, 451–454.

Mathews, J. H. 1987. *Numerical Methods for Mathematics, Science, and Engineering*. Prentice Hall, London.

Mawer, C. K. 1987. Shear criteria in the Grenville Province, Ontario, Canada. *J. Struct. Geol.* **9**, 531–539.

Nicolas, A. & Poirier, J. P. 1976. *Crystalline Plasticity of Solid State Flow in Metamorphic Rocks*. John Wiley and Sons, London

Oertel, G. 1965. Slow viscous flow of an incompressible suspension. *J. Eng. Mech. Div. ASCE* **91**, 145–154.

Passchier, C. W. 1994. Mixing in flow perturbations: a model for development of mantled porphyroclasts. *J. Struct. Geol.* **16**, 733–736.

Passchier, C. W. & Simpson, C. 1986. Porphyroclast systems as kinematic indicators. *J. Struct. Geol.* **8**, 831–844.

Passchier, C. W. & Sokoutis, D. 1993. Experimental modelling of mantled porphyroclasts. *J. Struct. Geol.* **15**, 895–909.

Passchier, C. W., ten Brink, C. E., Bons, P. D. & Sokoutis, D. 1993. δ objects as a gauge for stress sensitivity of strain rate in mylonites. *Earth Planet. Sci. Lett.* **120**, 239–245.

Poirier, J. P. 1985. *Creep of Crystals*. Cambridge University Press, Cambridge.

Simpson, C. & De Paor, D. 1993. Strain and kinematic analysis in general shear zones. *J. Struct. Geol.* **15**, 1–20.

ten Brink, C. E. & Passchier, C. W. 1995. Modelling of mantled porphyroclasts using non-Newtonian rock analogue materials. *J. Struct. Geol.* **17**, 131–146.

Tsenn, M. C. & Carter, N. L. 1987. Upper limits of power law creep of rocks. *Tectonophysics* **136**, 1–26.

Van Den Driessche, J. & Brun, J.-P. 1987. Rolling structures at large shear strain. *J. Struct. Geol.* **9**, 691–704.

Wakiya, S. 1956. Effect of a submerged object on a slow viscous flows: 2, a sphere in the flow between two parallel planes. *Res. Rep. Fac. Eng. Niigata Univ.* **5**, 1–12. (in Japanese)